Soft Matter

PAPER

Cite this: *Soft Matter*, 2018, **14**, 4603

Application of a constant hole volume Sanchez–Lacombe equation of state to mixtures relevant to polymeric foaming

Kier von Konigslow,[a] Chul B. Park [b] and Russell B. Thompson *[a]

Received 17th April 2018,
Accepted 6th May 2018

DOI: 10.1039/c8sm00794b

rsc.li/soft-matter-journal

A variant of the Sanchez–Lacombe equation of state is applied to several polymers, blowing agents, and saturated mixtures of interest to the polymer foaming industry. These are low-density polyethylene–carbon dioxide and polylactide–carbon dioxide saturated mixtures as well as polystyrene–carbon dioxide–dimethyl ether and polystyrene–carbon dioxide–nitrogen ternary saturated mixtures. Good agreement is achieved between theoretically predicted and experimentally determined solubilities, both for binary and ternary mixtures. Acceptable agreement with swelling ratios is found with no free parameters. Up-to-date pure component Sanchez–Lacombe characteristic parameters are provided for carbon dioxide, dimethyl ether, low-density polyethylene, nitrogen, polylactide, linear and branched polypropylene, and polystyrene. Pure fluid low-density polyethylene and nitrogen parameters exhibit more moderate success while still providing acceptable quantitative estimations. Mixture estimations are found to have more moderate success where pure components are not as well represented. The Sanchez–Lacombe equation of state is found to correctly predict the anomalous reversal of solubility temperature dependence for low critical point fluids through the observation of this behaviour in polystyrene nitrogen mixtures.

I. Introduction

Polymer foams are applied widely, from furniture to microelectronics.[1] While there exist many methods for foam production, one of the most widespread is based on driving mixtures of molten polymers and fluids into a supersaturated state in order to form gaseous voids in the polymer medium, then locking in the resulting structure by decreasing the temperature.[2,3] The polymers used in this method are known as thermoplastics, since they are capable of melting when heated.[1] The fluids used to create voids in the polymer medium are known as physical blowing agents (PBAs), since they are introduced to the polymer melt through physical mixing.[4]

The ability to predict the properties of these polymer–blowing agent mixtures is requisite for polymer foam processing.[3] To this end, the Sanchez–Lacombe equation of state (SL-EOS) has been invaluable in providing fluid phase equation of state information for the mixtures considered in polymer foaming.[5–8] The SL-EOS is a lattice fluid theory that includes lattice vacancies, known as "holes", to represent free volume.[6] The recent development of novel methods for the independent experimental measurement of solubility and swelling has shown that the SL-EOS performs poorly, even when the parameters are allowed to change with temperature and pressure.[9–12] Also, since the SL-EOS is the homogeneous limit of Hong–Noolandi Self-Consistent Field Theory (HN-SCFT)[13] poor performance of the SL-EOS on homogeneous polymer–solvent mixtures portends poor results for the application of HN-SCFT on inhomogeneous mixtures.[14–16]

In recent publications, we found that this poor performance was in part attributable to suboptimal regression procedures[17] and thermodynamic inconsistencies introduced by mixing rules.[18] As an alternative to mixing rules, we proposed a constant hole volume variant of the SL-EOS (ch-SL) that provides accurate phase equilibrium estimations for saturated polymer–solvent mixtures considered in the polymer foaming industry.[18] The idea of using a constant hole volume in the SL-EOS was first proposed by Panayiotou and Vera[19,20] and expanded upon by High and Danner.[21] In those works, the hole volume was set to a universal value of 9.75×10^{-3} m^3 kmol^{-1} which is the volume of a methylene group in polyethylene. In this work, the "constant" hole volume is a different constant for each mixture, reflecting all the different entropic and enthalpic interactions not captured by the statistical mechanics. The present ch-SL

[a] *Department of Physics & Astronomy and Waterloo Institute for Nanotechnology, University of Waterloo, 200 University Avenue West, Waterloo, Ontario, N2L 3G1, Canada. E-mail: thompson@uwaterloo.ca*
[b] *Department of Mechanical & Industrial Engineering, University of Toronto, 5 King's College Road, Toronto, Ontario, M5S 3G8, Canada*

was validated through its successful application to binary linear polypropylene (LPP) and branched polypropylene (BPP) and carbon dioxide (CO_2) mixtures.

The present work applies the ch-SL to several substances important to polymeric foaming: polystyrene (PS), polypropylene (PP), low-density polyethylene (LDPE), polylactide (PLA), carbon dioxide (CO_2), nitrogen (N_2) and dimethyl ether (DME). One of the first polymers to be successfully foamed, PS is an important polymer to the foaming industry since it exhibits excellent insulation properties and moisture resistance.[1] Polyolefin foams such as PP and LDPE are important to the building and packaging industries due to their low manufacturing costs,[1,22] despite their persistence in the environment.[23] In particular, PP is known for its high thermal stability and mechanical properties[24] whereas polyethylene materials, such as LDPE, exhibit high resilience and chemical resistance.[25] PLA is an encouraging candidate for a biodegradable replacement for petropolymers,[26,27] with PLA nanomaterials showing promise as scaffolding material in tissue engineering.[1] CO_2 is one of the most commonly used solvents in supercritical fluid extraction[28] and N_2 is one of the most commonly used reference fluids for physical models.[29] CO_2, N_2 and DME are desirable candidates for use as blowing agents since they are relatively abundant and less environmentally damaging than previously used fluids such as chlorofluorocarbons, hydrochlorofluorocarbons, or hydrofluorocarbons.[4,28–30]

II. Theory

Typically, a close-packed polymer–solvent system, such as a lattice construction of the Flory–Huggins type,[31] precludes the inclusion of pressure–volume effects. The Sanchez–Lacombe equation of state is derived from the assertion that there exists interstitial free volume between molecular cores, thus allowing for the inclusion of such effects. Rather than being merely treated as vacant, this space is partitioned into discrete entities of equal volume, which are treated as a distinct chemical species known as ''holes''. This species is associated with translational degrees of freedom, but has no interactions or internal degrees of freedom. In this way, it is assumed that all space is occupied either by molecular segments or holes, so that the system is treated as incompressible. By tuning the hole size, and thus the translational entropy, the holes are adjusted to correctly describe the pressure–volume–temperature (*PVT*) behaviour of the fluid. Based on this approach, a theory can be rigorously derived from first principles based on a coarse-grained Hamiltonian. This has been shown in detail from an off-lattice perspective in ref. 18. Here, we summarize the main features of this derivation.

The Helmholtz free energy, F, is obtained by substituting the canonical partition function, Q, under a mean field random mixture approximation into the relation $F = -k_B T \ln Q$, where k_B is Boltzmann's constant and T is the temperature.[18] The system is composed of n_κ molecules of each species κ, with n_0 referring to the number of artificial holes. Each molecule is divided into N_κ segments of equal volume v_κ so that each molecule occupies a volume $N_\kappa v_\kappa$. Holes are treated as trivial chains of length $N_0 = 1$ and volume given by v_0. For clarity, sums over all species κ with the superscript ''0'' include holes and those without the superscript exclude only holes. The expression for the free energy becomes[18]

$$\frac{F}{k_B T} = \frac{V}{v_r}\sum_{\kappa\kappa'}\frac{\varepsilon_{\kappa\kappa'}}{k_B T}\phi_\kappa\phi_{\kappa'} + \left[n_0 \ln\left(\frac{n_0 \Lambda_0^3}{V}\right) - n_0\right] + \sum_\kappa n_\kappa \ln\left(\frac{n_\kappa N_\kappa v_\kappa}{V}\right) \quad (1)$$

under the incompressibility constraint

$$\sum_\kappa^0 \phi_\kappa = 1. \quad (2)$$

Here, ϕ_κ is the volume fraction of species κ given by equation

$$\phi_\kappa = \frac{n_\kappa N_\kappa v_\kappa}{V}. \quad (3)$$

$\varepsilon_{\kappa\kappa'}$ is the interaction energy characterizing the interaction between κ and κ' segments, v_r is an arbitrary reference volume, V is the system volume, and Λ_0 is a normalization factor for the partition function, necessitated by the fact that holes are treated as a distinct chemical species. The incompressibility constraint in eqn (2) implies that the number of holes n_0 is not an independent thermodynamic variable, but rather a function of the total volume as well as the number of molecules.

Deriving the pressure from the Helmholtz free energy generates the equation of state. Pressure is related to the Helmholtz free energy through the relation $P = \left(\frac{\partial F}{\partial V}\right)_{T,\{n_\kappa\}}$, where the set $\{n_\kappa\}$ is taken to exclude n_0. The dimensionless pressure equation can be expressed as

$$\frac{v_r P}{k_B T} = -\sum_\kappa \left(\frac{1}{\alpha_0} - \frac{1}{\alpha_\kappa}\right)\phi_\kappa - \frac{1}{\alpha_0}\ln\phi_0 - \sum_{\kappa\kappa'}\frac{\varepsilon_{\kappa\kappa'}}{k_B T}\phi_\kappa\phi_{\kappa'} \quad (4)$$

where

$$\alpha_\kappa \equiv \frac{N_\kappa v_\kappa}{v_r} \quad (5)$$

represents the ratio of a molecular volume to the reference volume. The above equation of state makes use of the normalization factor $\Lambda_0^3 = v_0 e$, which is found to be necessary in order for the pressure to correctly vanish in the dilute limit.[13,18]

The equation of state given by eqn (4) was shown to be equivalent to the SL-EOS given the appropriate set of scaling parameters.[18] The SL-EOS is given by the equation

$$\tilde{\rho}^2 + \tilde{P} + \tilde{T}\left[\left(1 - \frac{1}{r}\right)\tilde{\rho} + \ln(1 - \tilde{\rho})\right] = 0 \quad (6)$$

where, from Sanchez and Lacombe,[6] the scaled variables of state are given by $\tilde{\rho} = \rho/\rho^* = V^*/V$, $\tilde{P} = P/P^*$, and $\tilde{T} = T/T^*$.

Each pure fluid κ is characterized by three molecular parameters and the molecular weight. These parameters are the interaction parameter $\varepsilon_{\kappa\kappa}$ describing the interaction of segments, the relative volume α_κ, as well as the hole volume $v_0^{(\kappa)}$. The superscript (κ) is necessary since the hole volume is assumed

to be a constant characteristic of a given species κ, differing for each species. These parameters are determined from comparison to experiment. Equivalently, the pure fluid can be characterized by thermodynamic reduced parameters. These parameters are the characteristic pressure P_κ^*, the characteristic temperature T_κ^*, and the characteristic density ρ_κ^*. They can be related to the molecular parameters through the relations

$$T_\kappa^* \equiv \frac{\varepsilon_{\kappa\kappa}}{k_B} \tag{7}$$

$$P_\kappa^* \equiv \frac{\varepsilon_{\kappa\kappa}}{v_0^{(k)}} \tag{8}$$

and

$$\rho_\kappa^* \equiv \frac{M_\kappa}{N_\kappa v_\kappa} \tag{9}$$

where M_κ is the molecular weight. Mixtures are characterized by the hole volume and the set of interspecies segment–segment interactions $\varepsilon_{\kappa\kappa'}$, where $\kappa \neq \kappa'$.

Comparing eqn (4) and (6), it can be shown that contact is made with SL-EOS with the definitions for the scaled density

$$\tilde{\rho} \equiv \sum_\kappa \phi_\kappa \tag{10}$$

and averaged interaction energy

$$\varepsilon^* \equiv \frac{1}{\tilde{\rho}^2} \sum_{\kappa\kappa'} \varepsilon_{\kappa\kappa'} \phi_\kappa \phi_{\kappa'}. \tag{11}$$

This allows the scaled temperature and pressure to be defined as before using $T^* = \varepsilon^*/k_B$ and $P^* = \varepsilon^*/v_0$, where v_0 is the hole volume of the mixture. Eqn (11) was derived by Sanchez and Lacombe as a necessary condition for a consistent cohesive energy density.[8] The only obstacle, therefore, to an internally consistent theory that limits correctly to describe each of the pure components is the hole volume v_0, which should take on the value $v_0^{(\kappa)}$ in each of the pure fluid limits. This has traditionally been accomplished using mixing rules on the hole volume, which requires only that the hole volume be a function of the pure fluid hole volumes, as well as the number of pure fluid molecules. Unlike the interaction energy mixing rule, the hole volume mixing rule is not derived, but is arbitrary in nature.[8]

It was found by Neau that chemical potentials derived from the configurational parition function in phases characterized by different hole volumes have different reference values, and thus cannot be consistently compared.[32] Although Neau proposed a solution to this using comparison of fugacities as an alternative to chemical potentials,[32] this is similarly inconsistent.[18] More significantly, this thermodynamic inconsistency is true for any mixing rules.[18]

The approach used here discards mixing rules in favour of a constant hole volume. There exist cases that do not require the theory to limit to the pure components. In principle, the constant hole should be chosen such that, at any composition, it is of a similar size as other segment species in order to exchange positions. Upon application of the mean field random mixing approximation however, the species are effectively treated as clumps of substance that displace holes, and so mixing rules for the holes designed to match the pure component segment sizes may not be needed for certain cases. Further discussion of this issue can be found in ref. 33. A constant hole volume can in fact be used along the line of saturation for polymer–solvent mixtures.[18] Excellent agreement was found with experimentally observed solubility in these cases without any additional parameters.[18] Despite using a constant hole volume, some inconsistency is unavoidable due to the comparison of chemical potentials in pure solvent and mixture phases using different hole volumes. This inconsistency is most noticeably manifest in the estimations of swelling, which are particularly vulnerable to differences in hole volumes in the pure polymer and mixture phases. Despite this, better than order-of-magnitude estimations of swelling are still possible.[18]

In order to calculate the composition of the saturated mixture, it is assumed that a solvent-rich and a polymer-rich phase are in thermal and diffusive equilibrium. A simplified phase equilibrium procedure is used, taking advantage of the nature of polymer–solvent systems used in polymer foaming. In polymer foaming, typical polymer–solvent saturation involves a solvent phase of fixed composition that is in coexistence with a polymer–solvent mixture phase. Since there will be no polymer vapour in the pure solvent phase, the volume fraction of polymer in that phase will be zero.[18] The equation of state allows for the calculation of the density of the pure solvent phase at fixed pressure P and temperature T. Knowing the density as well as composition allows for the calculation of the volume fractions and chemical potentials of the solvents in the solvent phase. Diffusive equilibrium implies that the chemical potentials of each solvent species are equal in both the pure solvent and mixture phases. Nonlinear solving techniques are used to simultaneously and numerically solve the equation of state and solvent chemical potential expressions in the mixture phase to determine the volume fractions of all species in the mixture.

Experimentally observed mixture data take the form of solubility and swelling. Corresponding quantities are calculated from the theory in order to compare with experiment. The solubility of a saturated polymer–solvent mixture is defined to be the fraction of the mass of solvent to the total mass. The solubility of the solvent species κ is defined

$$\chi_\kappa = \frac{M_\kappa \phi_\kappa / \alpha_\kappa}{\sum_{\kappa'} M_{\kappa'} \phi_{\kappa'} / \alpha_{\kappa'}} \tag{12}$$

where all volume fractions are calculated in the mixture phase at saturation. For mixtures containing multiple solvents, the solubility is defined to be

$$\chi = \sum_s \chi_s \tag{13}$$

where the sum over s is taken to be the sum over all solvents present in the mixture phase. Swelling is defined to be the ratio of the volume of the mixture to the volume of the pure polymer.

From eqn (3) under the constraint that the pure polymer and mixture phases identically contain n_κ polymer molecules, the swelling ratio is given by the relation

$$S_W = \frac{V_{mix}}{V_{polymer}} = \frac{\phi_\kappa^{pure}}{\phi_\kappa^{mix}}. \quad (14)$$

This equation is appropriate for all mixtures containing a single polymer species.

All parameters are determined from experimentally obtained data. Pure fluid parameters are obtained from pure fluid *PVT* data in the gaseous, liquid, and supercritical regime where available. Carbon dioxide includes saturated vapour pressure data from the triple point to near the critical point. Data within 1.5 MPa and 15.0 K of the critical point are excluded.[17] Regression is performed using a nonlinear least-squares fit to pressure data, using a Levenberg–Marquardt algorithm for optimization.[34,35] Mixture parameters are determined from nonlinear least-squares regression of solubility data using the same optimization procedure.

III. Results and discussion

In Fig. 1 and 2, the experimentally measured solubility and swelling of saturated PLA/CO_2 and LDPE/CO_2 mixtures are compared with theoretical curves based on the ch-SL theory. Experimental data was obtained from Mahmood *et al.*[41] for PLA/CO_2 and Hasan[37] for LDPE/CO_2. Pure fluid parameters were regressed from experimental *PVT* data, with constant parameters assumed for all pressures and temperatures. Supercritical *PVT* and vapour pressure data were included in the parameter estimation where such data was available. The characteristic parameters for the pure fluids as well as the sources of the pure fluid experimental data are found in Table 1.

All mixture parameters were regressed from experimental solubility data assuming constant parameters over all temperatures and pressures. Swelling data was not included in the regression because inconsistent hole volumes between phases could negatively affect the quality of the fit, although previous attempts to include swelling in the regression did not improve the quality of the fit.[18] Just as in the pure fluid, fitting was performed using a nonlinear least-squares algorithm. The binary interaction parameters resulting from the regression are found in Table 2 and the hole volumes characteristic of the binary phases are found in Table 3.

Comparing Fig. 1(a) with Fig. 2(a), it appears that while the theory performs qualitatively well for both the saturated PLA/CO_2 and LDPE/CO_2 mixtures, there is a marginal difference in their degree of agreement with experiment. In both cases, the theoretical curves produce estimates in the correct range of solubilities, but the PLA/CO_2 mixture produces slightly better agreement with the overall trend, whereas LDPE/CO_2 appears to underestimate the solubility at high pressures.

This difference is likely not attributable to the disparity in hole volumes between the pure fluids. Table 3 lists the hole volumes characteristic of the pure fluids and mixtures. Given that the hole volume of CO_2 is closer to LDPE than to either BPP or LPP, one would expect LDPE to perform better than either. Instead, the BPP/CO_2 and LPP/CO_2 mixtures appear qualitatively to yield better fits.[18] This is because polymer hole volumes do not enter into calculation of diffusive equilibrium or of solubility. Another explanation suggests itself when cross-referencing the solubility plots with the comparisons of experimental and theoretical densities for PLA and LDPE melts in Fig. 3. Experimental data for the pure fluid densities in Fig. 3 was obtained from Sato *et al.*[38] for PLA, and from Hasan[37] for LDPE. The theoretical density isotherms for PLA in Fig. 3(a) agree with experiment much better than the ones for LDPE in Fig. 3(b). It is possible that the relatively poorer performance of LDPE/CO_2 can be explained by the deficient estimations made by the pure fluid parameters. This is consistent with the result found by Bashir *et al.*[44] that the pure fluid characteristic parameters can have a profound effect on the validity of the multicomponent fluid theory. In a previous publication, we found that the pure fluid characteristic parameters can greatly benefit from regression performed over a larger

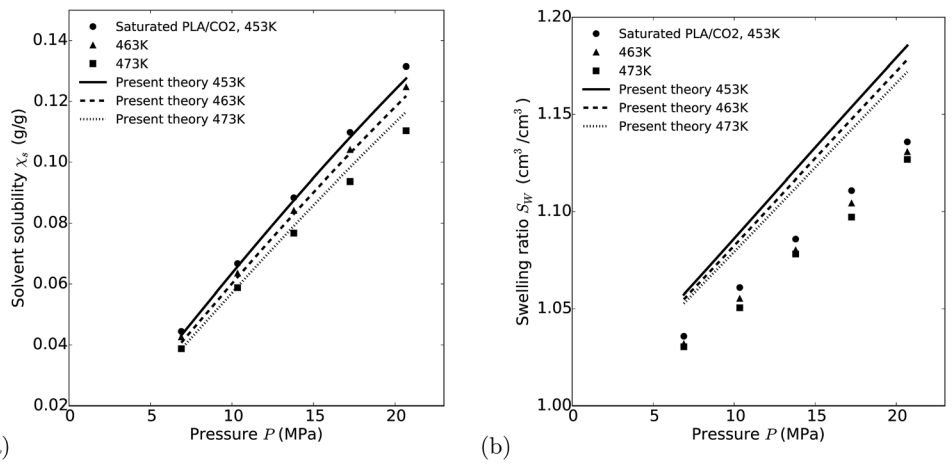

Fig. 1 A comparison of experimental and theoretical (a) solubility and (b) swelling for saturated binary PLA/CO_2 mixtures at various temperatures. Points are experimental data and lines are fits based on the present theory as denoted by the legends.

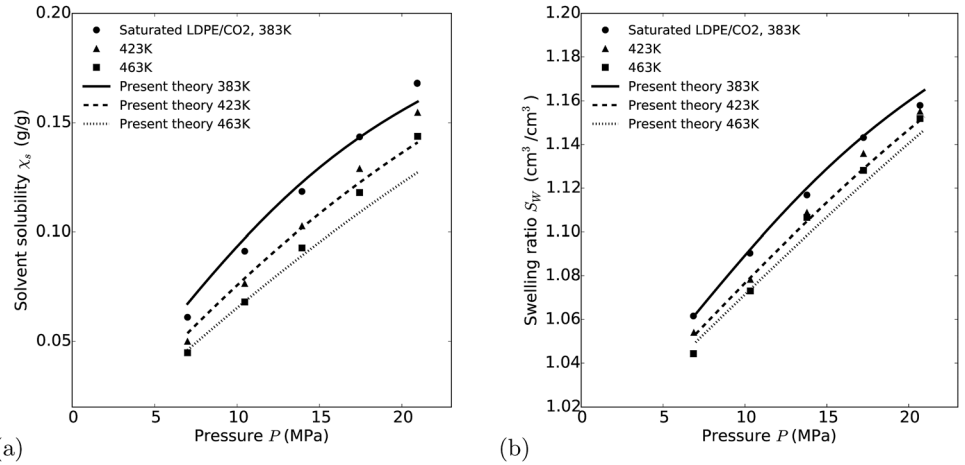

Fig. 2 A comparison of experimental and theoretical (a) solubility and (b) swelling for saturated binary LDPE/CO_2 mixtures at various temperatures. Points are experimental data and lines are fits based on the present theory as denoted by the legends.

Table 1 A list of the pure fluid characteristic parameters determined from experimental *PVT* data. The sources of the experimental data are indicated in the last column

Pure fluid	P^* (MPa)	T^* (K)	ρ^* (g cm^{-3})	P (MPa)	T (K)	Data source
CO_2	419.9	341.8	1.397	0.5–66.57	216.58–1800.0	Refer to ref. 17
DME	313.8	450.0	0.8146	0.01–164.8	423.0–543.0	36
LDPE	407.5	586.6	0.9271	0.01–0.927	393.0–453.0	37
N_2	178.5	103.7	1.128	0.01–1000.0	135.0–650.0	29
PLA	598.4	617.3	1.347	0.1–200.0	453.4–493.3	38
BPP	356.4	656.0	0.8950	0.5–65.0	453.0–493.0	39
LPP	316.2	662.8	0.8685	0.5–65.0	453.0–493.0	39
PS	421.8	687.8	1.118	0.01–200.0	402.65–524.45	40

Table 2 A list of the binary interaction parameters for each pair of mixture components and their corresponding sources of experimental data

Binary mixture	ζ	v_0 (10^{-24} cm^3)	P (MPa)	T (K)	Data source
LDPE/CO_2	0.9680	10.48	7.0–21.0	383.0–463.0	37
PLA/CO_2	1.046	9.883	6.9–20.7	453.0–473.0	42
BPP/CO_2	1.091	8.646	7.0–31.4	453.0–493.0	37
LPP/CO_2	1.110	8.436	7.0–31.4	453.0–493.0	37
PS/CO_2	1.021	9.900	6.7–20.6	403.0–463.0	37
PS/DME	1.006	18.08	0.3–4.95	423.0–483.0	43
PS/N_2	1.346	8.769	6.9–20.9	403.0–463.0	37

Table 3 A list of the hole volumes v_0 characteristic of each of the pure, binary mixture, and ternary mixture fluids

Fluid		v_0 (10^{-24} cm^3)
Pure fluid	CO_2	11.24
	DME	19.80
	LDPE	19.87
	N_2	8.021
	PLA	14.24
	BPP	25.41
	LPP	28.94
	PS	22.51
Binary mixture	LDPE/CO_2	10.48
	PLA/CO_2	9.883
	BPP/CO_2	8.646
	LPP/CO_2	8.436
	PS/CO_2	9.900
	PS/DME	18.08
	PS/N_2	8.769
Ternary mixture	PS/CO_2 + DME	16.74
	PS/CO_2 + N_2	8.628

thermodynamic range,[17] proposing possible improvement for future consideration.

On the other hand, the theory performs unexpectedly well for LDPE/CO_2 in terms of swelling, especially at lower temperature. This is despite the fact that swelling was not included in the considerations for fitting. More puzzling, a comparison of the dissimilarity of hole volumes in Table 4 shows that the PLA hole volume is much closer to that of CO_2 ($\sim$27%) than that of LDPE ($\sim$77%). One would expect that swelling calculations would become more accurate as the polymer and solvent hole volumes became more similar, rather than the converse.

The swelling ratio, defined as the ratio of the volume of the saturated polymer–solvent mixture to the volume of the polymer sample, is given by eqn (14). Fig. 4(a) and (b) compare the experimentally determined swelling ratios to theoretical ratios calculated under the assumption that the reference volume of the initial polymer sample is pure. In practice, however, the polymer sample is not pure, but contains solvent molecules corresponding to air. Since N_2 forms the largest component of air, it is possible to partially compensate for the presence of these solvents by including the N_2 molecules contained in the polymer sample under approximate laboratory conditions (298 K and 0.101 MPa). Fig. 4(c) and (d) compare the experimentally determined swelling ratios to theoretical ratios calculated assuming that the polymer sample contains no air. The effect of this compensation is to decrease the swelling ratios predicted by the theory. While this effect is significant in the PS/N_2 mixtures, the effect is minimal in the PS/CO_2 mixtures due to the relatively low solubility of N_2 in PS. Given the greatly increased complexity, considering the contribution of air to the polymer sample is therefore not justified, except in mixtures featuring very low solubilities.

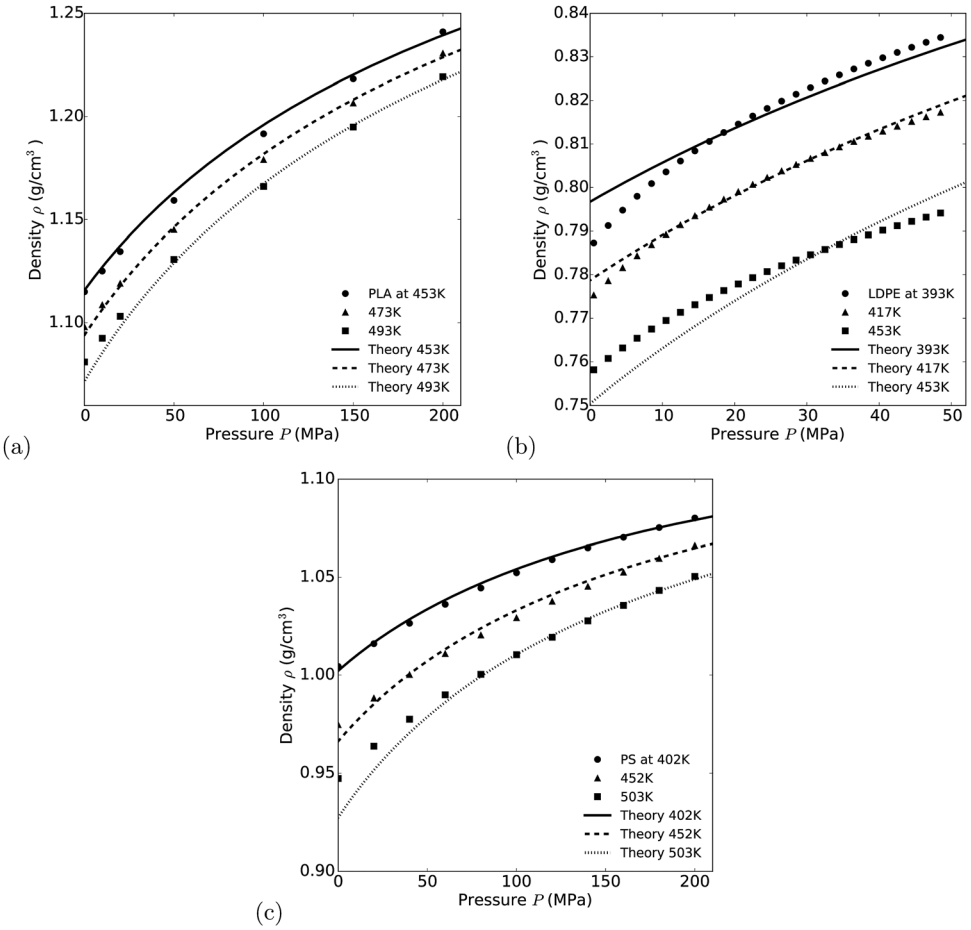

Fig. 3 A comparison of experimental and theoretical density isotherms for (a) PLA, (b) LDPE, and (c) PS. Points are experimental data and lines are fits based on the present theory as denoted by the legends.

Table 4 A comparison of the CO_2 hole volume v_0 to those of pure PLA and LDPE as well as saturated binary PLA/CO_2 and PLA/CO_2 mixtures

Fluid	v_0 (10^{-24} cm^3)
CO_2	11.24
PLA	14.24 (26.70%)
PLA/CO_2	9.883 (12.07%)
LDPE	19.87 (76.78%)
LDPE/CO_2	10.48 (8.30%)

In order to place the performance of the ch-SL theory into context, we follow the example of Nies and Stroeks[45,46] who compared a variant of the Simha–Somcynsky model to the traditional Simha–Somcynsky EOS. In our case, we compare the performance of the constant hole SL-EOS with the traditional SL theory that uses mixing rules, specifically, the one-parameter mixing rule used originally by Sanchez and Lacombe[7] and a two-parameter mixing rule as given by Poser and Sanchez.[47] The results are shown in Fig. 5. In all but one case, the constant hole SL-EOS is quantitatively superior to the traditional SL-EOS using either mixing rule. The exception is the solubility of nitrogen in polystyrene, which is not surprising since, as already discussed, the pure component parameters for nitrogen do not perform as well as the pure component parameters for other substances, and therefore the mixture results will be less reliable. In any case, the three EOS solubility fits for nitrogen in Fig. 5(e) are all very close to each other and to the experimental data, so the constant hole volume approach is still in excellent agreement with experiment.

In Fig. 6 and 8, the multicomponent fluid theory is successfully applied to PS/CO_2 + DME and PS/CO_2 + N_2 ternary mixtures. In both cases a solvent mixture of fixed composition, for example CO_2 and DME, is put into contact with a polymer, in this case PS, until diffusive equilibrium is reached. Experimental data was obtained from Mahmood *et al.*[12,41] for PS/CO_2 + DME and from Hasan[37] for PS/CO_2 + N_2. In ternary and higher-order mixtures, solubility is defined as the total solubility of solvent in the mixture rather than the solubility of a single component.

Fig. 6 illustrates the experimental and corresponding theoretical solubility data for a PS/CO_2 + DME saturated mixture under a variety of conditions. Fig. 6(a) shows this comparison for a 90 : 10 CO_2 : DME ratio at a variety of temperatures and Fig. 6(b) shows the mixture at 423 K for a variety of ratios. The latter figure exhibits a trend of increasing solubility with increasing initial concentrations of DME in agreement with experiment. While it is unfortunately not possible to experimentally

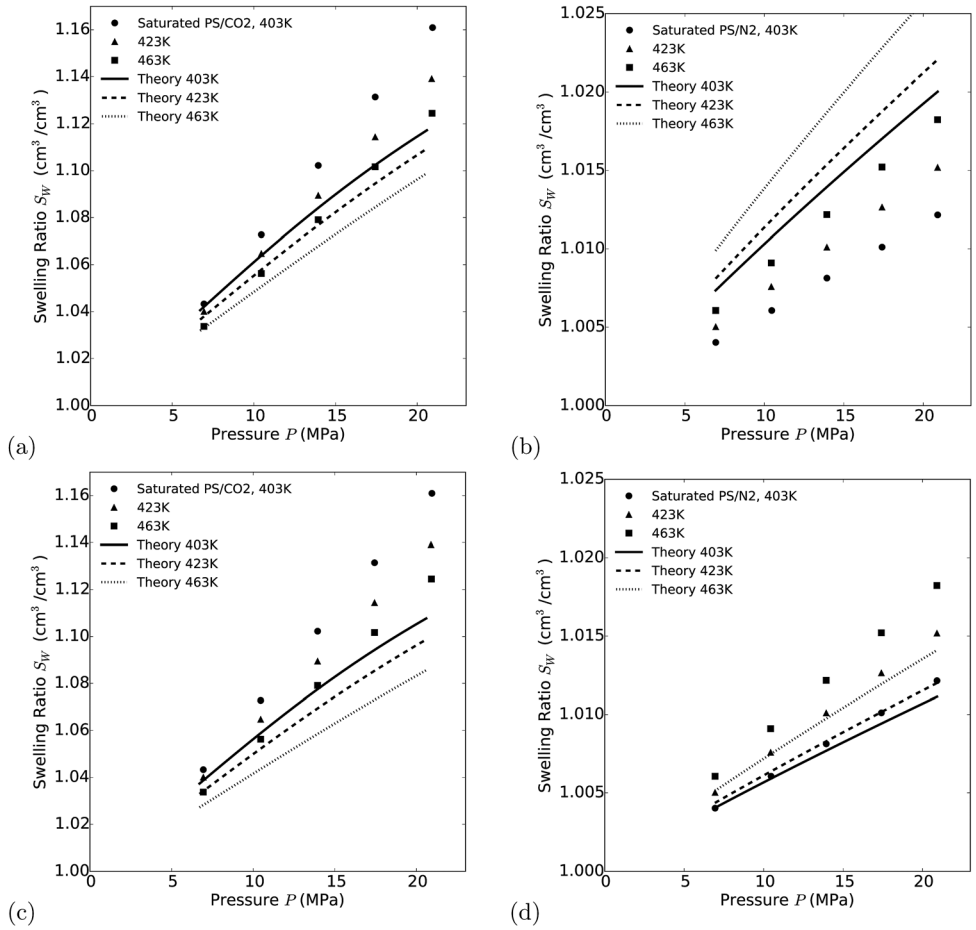

Fig. 4 A comparison of experimental and theoretical swelling ratios for saturated (a) PS/CO_2 and (b) PS/N_2 mixtures at various temperatures assuming the reference polymer sample is pure. A comparison of experimental and theoretical swelling ratios for saturated (c) PS/CO_2 and (d) PS/N_2 mixtures at various temperatures assuming the reference polymer sample contains air (N_2). Points are experimental data and lines are fits based on the present theory as denoted by the legends.

determine the solubilities of the individual components due to current technical limitations, they can be theoretically calculated by regressing the mixture parameters from the total solubility, then using phase equilibrium calculations to predict the corresponding system composition. Using a similar approach, it has been deduced from the Simha–Somcynsky (SS) equation of state that an increase in the initial concentration of DME corresponds to an increase in the solubility of CO_2 in the mixture.[41] Fig. 6(c) shows the ch-SL predicted solubility of CO_2 in the mixture for various initial concentrations of DME. Unlike the SS-based calculation, the ch-SL result shows decreasing CO_2 solubility with increasing DME. Taken together, Fig. 6(b) and (c) imply that, according to ch-SL, increasing concentrations of DME are akin to replacement of CO_2 with a solvent with more of an affinity for PS. This conclusion seems to be supported by the observation in Fig. 6(b) that the total solvent solubility increases with the concentration of DME, reaching a maximum for 0 : 100 CO_2 : DME solvent ratios. While the pressure ranges of the binary PS/DME and ternary PS/CO_2 + DME experiments do not overlap, it is nevertheless possible to observe that the solubility of DME near 5 MPa is higher than CO_2 near 7 MPa. One can therefore infer from the experimental data that the solubility of DME in PS is greater than that of CO_2.

In Fig. 6(b), as the ratio of CO_2 : DME is increased to 100 : 0 the theory begins to deviate significantly from experiment. This is to be expected, since the hole volume characterizing the binary PS/CO_2 mixture is not equal to that characterizing the ternary PS/CO_2 + DME mixture. Since even the 90 : 10 ratio agrees well with experiment, it appears that the transition between the two characters of fluid is quite sharp. The same deviation from experiment is not seen as the ratio is decreased to 0 : 100, corresponding to the binary PS/DME mixture. This is likely the result of the relative similarity between the hole volumes characterizing binary PS/DME mixtures, regressed from the binary PS/DME mixtures shown in Fig. 7, and the ternary PS/CO_2 + DME mixtures. The hole volumes corresponding to these mixtures can be found in Table 3.

Fig. 8 corresponds to saturated mixtures of PS/CO_2 + N_2. While good qualitative agreement is achieved overall, it is observed that the correspondence of experimental and theoretical solubility worsens with increasing concentration of N_2. This could be due to the poor agreement between experiment, derived from the

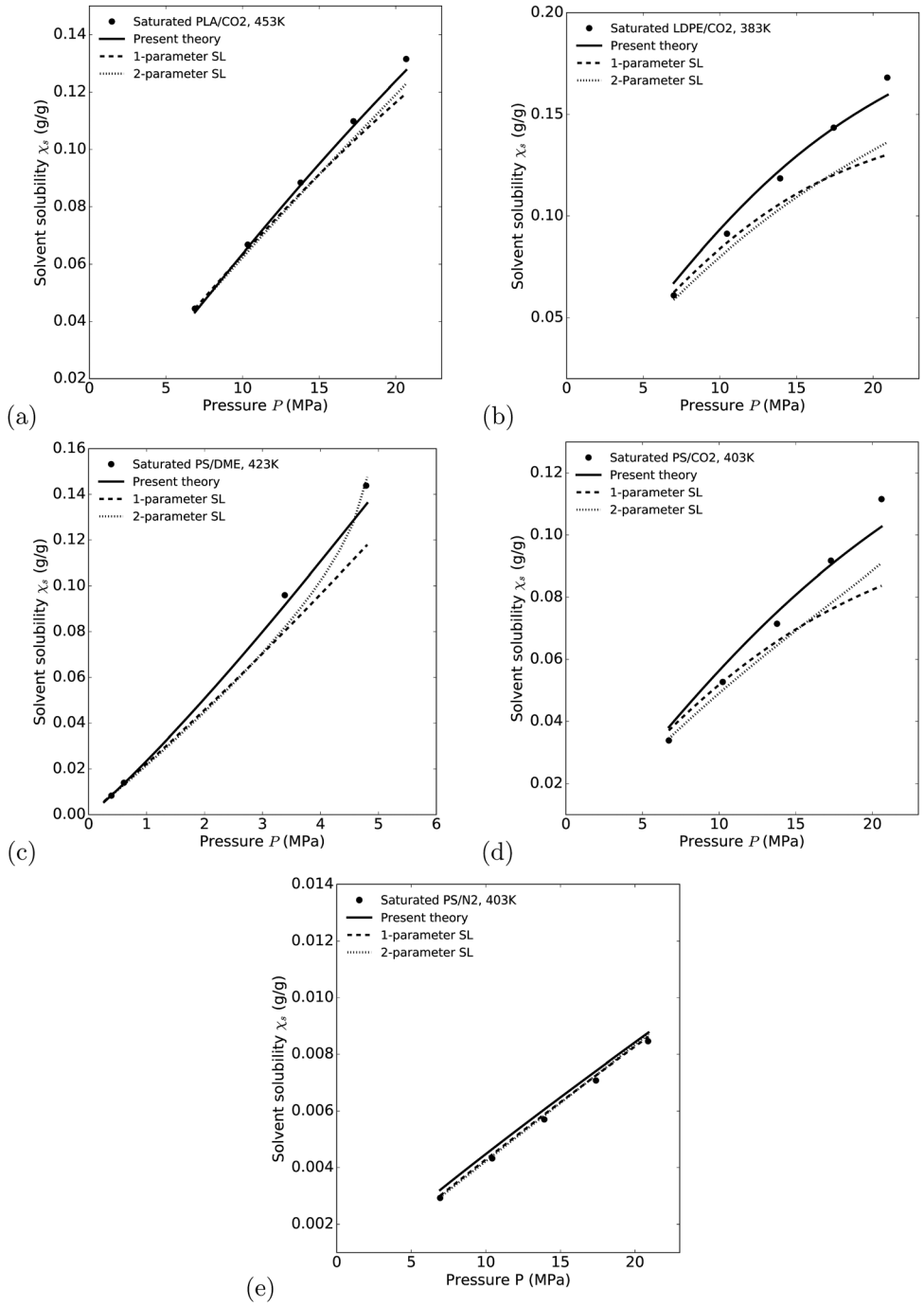

Fig. 5 A comparison of experimental and theoretical solubilities for (a) PLA/CO_2 at 453 K (b) LDPE/CO_2 at 383 K (c) PS/DME at 423 K (d) PS/CO_2 at 403 K and (e) PS/N_2 at 403 K. Points are experimental data and lines are fits based on theories as denoted by the legends.

empirical equation of state determined by Span *et al.*,[29] and theory for pure N_2, contrasted with the excellent agreement for CO_2. The reason for this is unknown, but it is of note that the pure fluid interaction parameter, derived from the characteristic parameters, is by far weaker in N_2 than it is for any of the other fluids here considered. It is also the fluid with the smallest hole volume, as seen in Table 3, meaning that the hole volume disparity is greatest when considering mixtures of N_2 with other fluids. It is possible that N_2, being somewhat anomalous in that it has such a low solubility, requires additional model considerations absent from SL.

Mixtures containing N_2 and other gases with low critical temperatures have been known to show unusual temperature dependence in solubility, with solubility increasing with temperature.[37] In many other saturated mixtures, the solubility of a solvent decreases with temperature.[30,42] Fig. 9 compares experimental and theoretical solubility for saturated mixtures of PS/CO_2 and PS/N_2. Experimental data for both plots was taken from Hasan.[37] A comparison of

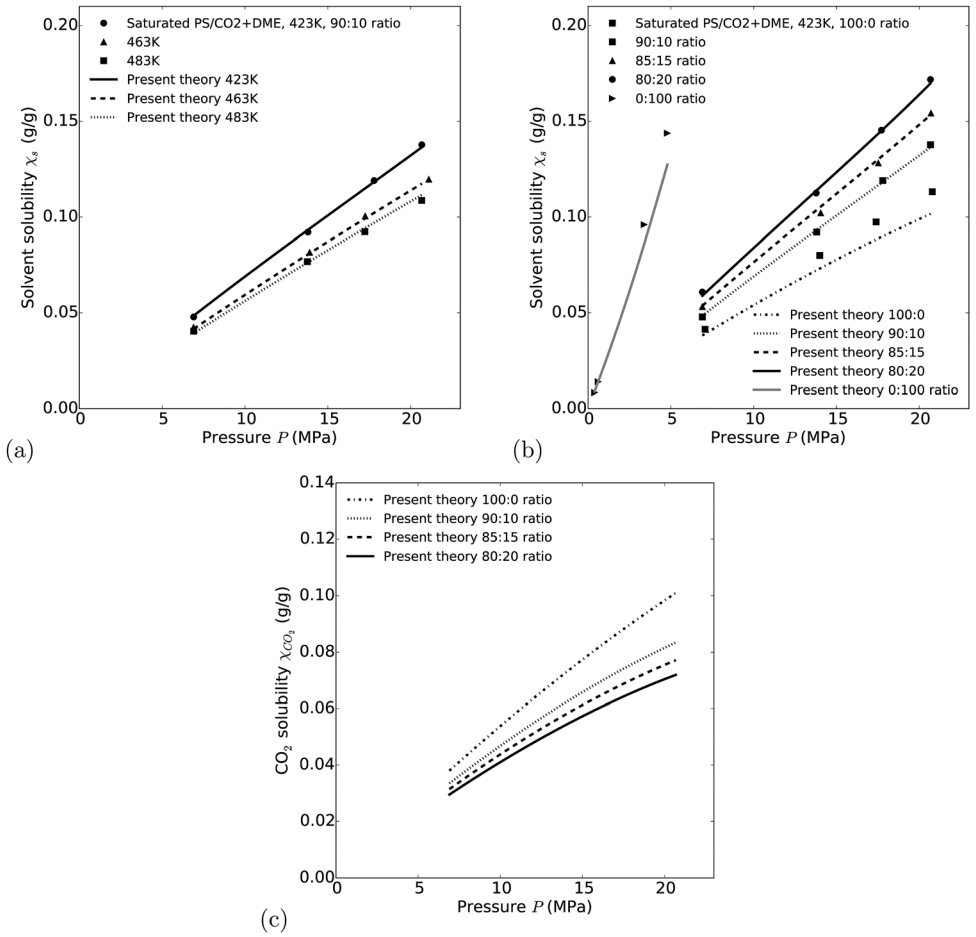

Fig. 6 A comparison of experimental and theoretical solvent solubility for saturated ternary PS/CO_2 + DME mixtures at various (a) temperatures and (b) solvent ratios. A plot of theoretical CO_2 solubility (c) at various solvent ratios. Points are experimental data and lines are fits based on the present theory as denoted by the legends.

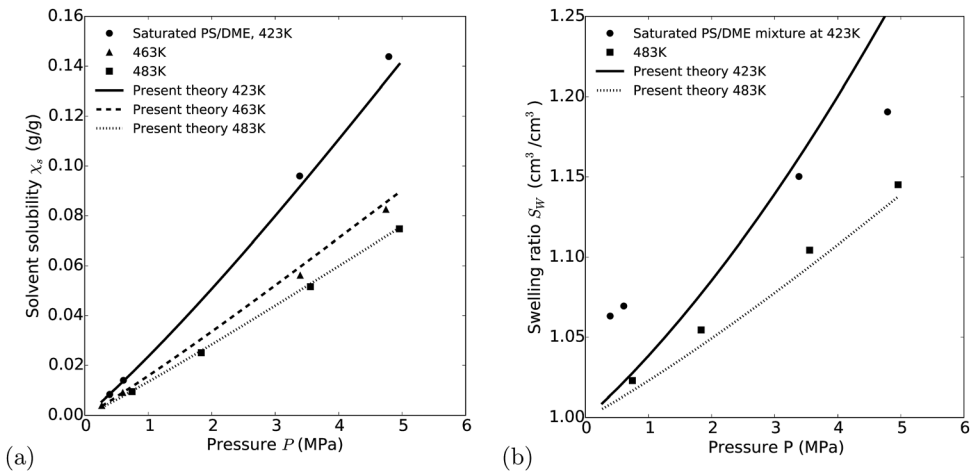

Fig. 7 A comparison of experimental and theoretical (a) solubility and (b) swelling at various temperatures for saturated PS/DME mixtures. Points are experimental data and lines are fits based on the present theory as denoted by the legends.

Fig. 9a and b shows that, while PS/CO_2 exhibits decreasing solubility with temperature, it is reversed in the PS/N_2 mixture. This is reproduced in the theory, with the fitted curves showing the same temperature dependence anomaly. In the ternary PS/CO_2 + N_2 saturated mixture, decreasing the CO_2 : N_2 ratio decreases the total solubility, illustrated in Fig. 8. Fig. 9b, corresponding to

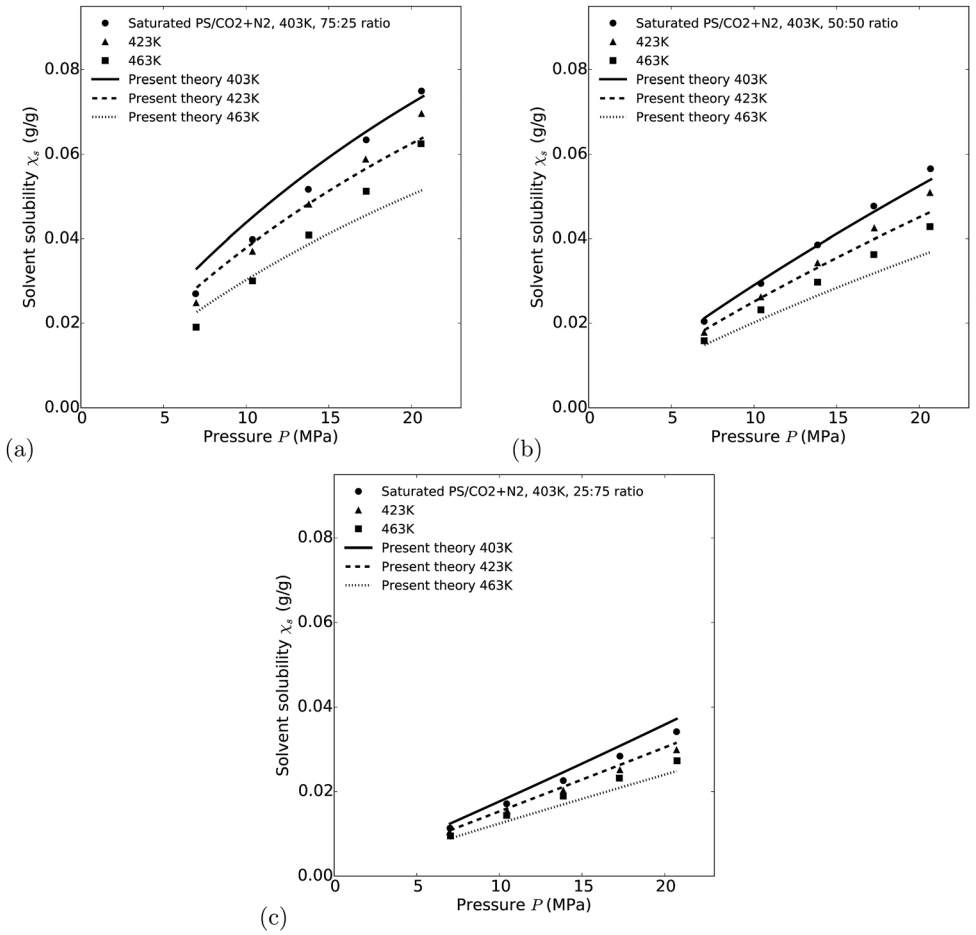

Fig. 8 A comparison of experimental and theoretical solubility for saturated PS/CO_2 + N_2 mixtures at various temperatures for CO_2 : N_2 solvent ratios of (a) 75 : 25, (b) 50 : 50, and (c) 25 : 75. Points are experimental data and lines are fits based on the present theory as denoted by the legends.

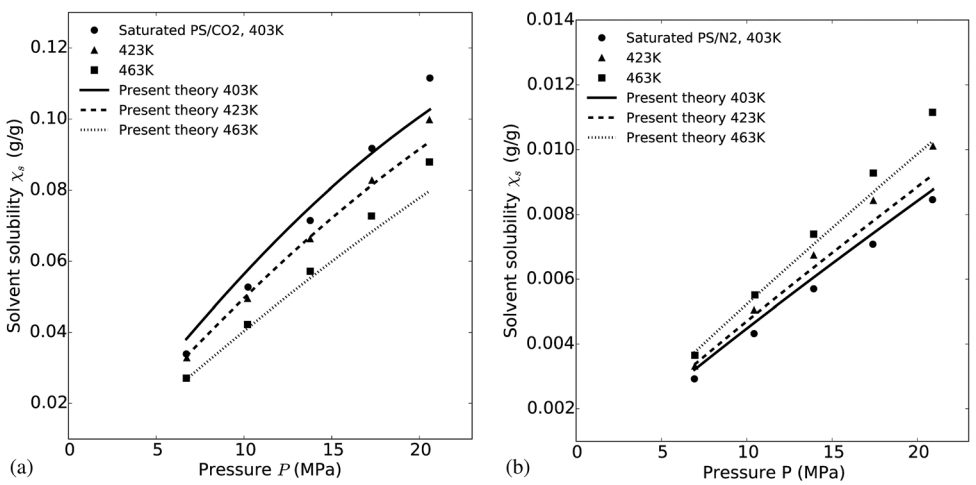

Fig. 9 A comparison of experimental and theoretical solubility at various temperatures for saturated (a) PS/CO_2 and saturated (b) PS/N_2 mixtures. Points are experimental data and lines are fits based on the present theory as denoted by the legends.

the 0 : 100 ratio, has not only a much lower solubility, but also a reversed temperature dependence as expected.

Table 3 lists the hole volumes regressed from experiment. A noticeable pattern appears from the mixtures, both binary and ternary. While the hole volumes tend to be larger for the macromolecules than for the solvents, the hole volumes of the mixtures tend to be more strongly influenced by those of the solvents. This may be in part due to the fact that, after a

certain size, further increase in molecular weight of polymers ceases to have as much effect on solubility. For ternary systems, one might be concerned that the presence of two solvents of different hole volumes would impair solubility calculations. Application of the theory to ternary systems does not bear this out, however, since good agreement with solubility is achieved. In these fluids, the mixture hole volume appears to lie between those of the two solvents. It may be possible to take advantage of these hole volume observations to estimate the hole volume characteristic of the mixture by a comparison of the hole volumes of the constituents, greatly simplifying mixture parameter estimation.

It should be noted that these patterns do not appear strict and are subject to exceptions. For example, while the solvent hole volumes are as a rule smaller than those of the polymers, the hole volume associated with DME is larger than that of PLA and comparable to that of LDPE. These exceptions introduce ambiguity that could provide alternate interpretations of the observed patterns. For example, in the ternary mixtures the hole volume associated with the PS/CO_2 + N_2 is comparable to the hole volume of the smallest solvent hole volume, whereas the hole volume associated with PS/CO_2 + DME is larger than those of the solvent molecules. An alternative interpretation of the observed pattern is that the hole volumes associated with mixtures are dominated by those of the smallest solvent hole volume, with the PS/CO_2 + DME mixture as a possible exception.

IV. Conclusions

The SL-EOS is applied to pure DME, LDPE, N_2, PLA, and PS fluids as a necessary preliminary step to consideration of their mixtures. Of these, it is found that all exhibit excellent agreement with experiment with only moderately less success for pure LDPE and pure N_2, where the reason for the relatively poorer performance of the theory for these fluids is not yet known. Even with this more moderate success for LDPE and N_2 pure fluids, the theory still yields acceptable quantitative results. Pure component parameters for all of the fluids are given.

The ch-SL is applied to binary LDPE/CO_2 and PLA/CO_2 as well as ternary PS/CO_2 + DME and PS/CO_2 + N_2 saturated mixtures. Good agreement between theoretically calculated and experimentally measured solubility provides further validation for the ch-SL, with mixture parameters proposed for each of the mixtures. While only moderate agreement with experimental swelling is observed, this is consistent with our previous observation that calculations comparing a polymer-rich phase, a solvent-rich phase, and a mixture phase that have disparate hole volumes skews swelling estimations. In addition, comparison of the quality of theoretical solubility estimations to the quality of pure component *PVT* estimations for both LDPE/CO_2 and PLA/CO_2 mixtures show the impact of pure fluid characteristic parameters on fluid mixture results. Together, these observations provide evidence for our previous proposal that the poor correlation of the SL-EOS to experimentally obtained solubility is due in part to suboptimal regression and a thermodynamic inconsistency introduced by mixing rules. Further, the SL-EOS is found to correctly predict the anomalous temperature dependence of solubility exhibited by low critical point solvents by exhibiting a reversed solubility temperature dependence in binary PS/N_2 and ternary PS/CO_2 + N_2 saturated mixtures.

Conflicts of interest

There are no conflicts to declare.

Acknowledgements

This research was financially supported by the Natural Sciences and Engineering Research Council of Canada under the Discovery Grant programme and by the Consortium for Cellular and Microcellular Plastics (CCMCP) at the University of Toronto.

References

1 E. Aram and S. Mehdipour-Ataei, *Int. J. Polym. Mater. Polym. Biomater.*, 2016, **65**, 358.
2 C. Okolieocha, D. Raps, K. Subramaniam and V. Altstädt, *Eur. Polym. J.*, 2015, **73**, 500.
3 A. Primel, J. Férec, G. Ausias, Y. Tirel, J.-M. Veillé and Y. Grohens, *J. Supercrit. Fluids*, 2017, **122**, 52.
4 L. J. M. Jacobs, M. F. Kemmere and J. T. F. Keurentjes, *Green Chem.*, 2008, **10**, 731.
5 I. C. Sanchez and R. H. Lacombe, *Nature*, 1974, **252**, 381.
6 I. C. Sanchez and R. H. Lacombe, *J. Phys. Chem.*, 1976, **80**, 2352.
7 R. H. Lacombe and I. C. Sanchez, *J. Phys. Chem.*, 1976, **80**, 2568.
8 I. C. Sanchez and R. H. Lacombe, *Macromolecules*, 1978, **11**, 1145.
9 M. M. Hasan, Y. G. Li, G. Li, C. B. Park and P. Chen, *J. Chem. Eng. Data*, 2010, **55**, 4885.
10 Y. G. Li, C. B. Park, H. B. Li and J. Wang, *Fluid Phase Equilib.*, 2008, **270**, 15.
11 Y. G. Li and C. B. Park, *Ind. Eng. Chem. Res.*, 2009, **48**, 6633.
12 S. H. Mahmood, C. L. Xin, J. H. Lee and C. B. Park, *J. Colloid Interface Sci.*, 2015, **456**, 174.
13 K. M. Hong and J. Noolandi, *Macromolecules*, 1981, **14**, 1229.
14 Y. Kim, C. B. Park, P. Chen and R. B. Thompson, *Soft Matter*, 2011, **7**, 7351.
15 Y. Kim, C. B. Park, P. Chen and R. B. Thompson, *Polymer*, 2011, **52**, 5622.
16 Y. Kim, C. B. Park, P. Chen and R. B. Thompson, *Polymer*, 2013, **54**, 841.
17 K. von Konigslow, C. B. Park and R. B. Thompson, *J. Chem. Eng. Data*, 2017, **62**, 585.
18 K. von Konigslow, C. B. Park and R. B. Thompson, *Phys. Rev. Appl.*, 2017, **8**, 044009.
19 C. Panayiotou and J. H. Vera, *Polym. Eng. Sci.*, 1982, **22**, 345.
20 C. Panayiotou and J. H. Vera, *Polym. J.*, 1982, **14**, 681.

21 M. S. High and R. P. Danner, *Fluid Phase Equilib.*, 1989, **53**, 323.
22 D. W. Sauter, M. Taoufik and C. Boisson, *Polymers*, 2017, **9**, 185.
23 J. Saleem, M. Adil Riaz and G. McKay, *J. Hazard. Mater.*, 2018, **341**, 424.
24 C. Yang, Z. Xing, Q. Zhao, M. Wang and G. Wu, *J. Appl. Polym. Sci.*, 2018, **135**, 45809.
25 S.-T. Lee, C. B. Park and N. S. Ramesh, *Polymeric Foams: Science and Technology*, CRC Taylor and Francis, Boca Raton, FL, 2007.
26 M. Nofar and C. B. Park, *Prog. Polym. Sci.*, 2014, **39**, 1.
27 J.-M. Raquez, Y. Habibi, M. Murariu and P. Dubois, *Prog. Polym. Sci.*, 2013, **38**, 1504.
28 R. Span and W. Wagner, *J. Phys. Chem. Ref. Data*, 1996, **25**, 1509.
29 R. Span, E. W. Lemmon, R. T. Jacobsen, W. Wagner and A. Yokozeki, *J. Phys. Chem. Ref. Data*, 2000, **29**, 1361.
30 Y. Sato, M. Yurugi, K. Fujiwara, S. Takishima and H. Masuoka, *Fluid Phase Equilib.*, 1996, **125**, 129.
31 P. J. Flory, *J. Chem. Phys.*, 1944, **12**, 425.
32 E. Neau, *Fluid Phase Equilib.*, 2002, **203**, 133.
33 K. von Konigslow, *An off-lattice derivation and thermodynamic consistency consideration for the Sanchez–Lacombe equation of state*, PhD thesis, University of Waterloo, 2017.
34 D. W. Marquardt, *J. Soc. Ind. Appl. Math.*, 1963, **11**, 431.
35 S. J. Ahn, *Lecture Notes in Computer Science*, Springer Berlin Heidelberg, Berlin, Heidelberg, 2004.
36 J. Wu, Y. Zhou and E. W. Lemmon, *J. Phys. Chem. Ref. Data*, 2011, **40**, 023104.
37 M. M. Hasan, *A Systematic Study of Solubility of Physical Blowing Agents and Their Blends in Polymers and Their Nanocomposites*, PhD thesis, School University of Toronto, 2013.
38 Y. Sato, K. Inohara, S. Takishima, H. Masuoka, M. Imaizumi, H. Yamamoto and M. Takasugi, *Polym. Eng. Sci.*, 2000, **40**, 2602.
39 G. Li, J. Wang, C. B. Park and R. Simha, *J. Polym. Sci., Part B: Polym. Phys.*, 2007, **45**, 2497.
40 P. Zoller and D. J. Walsh, *Standard Pressure–Volume–Temperature Data for Polymers*, Technomic Publishing Company, 1995.
41 S. H. Mahmood, C. L. Xin, P. Gong, J. H. Lee, G. Li and C. B. Park, *Polymer*, 2016, **97**, 95.
42 S. H. Mahmood, M. Keshtkar and C. B. Park, *J. Chem. Thermodyn.*, 2014, **70**, 13.
43 S. H. Mahmood, *Thermodynamic Investigation of the Interaction between Polymer and Gases*, PhD thesis, University of Toronto, 2017.
44 M. A. Bashir, M. Al-haj Ali, V. Kanellopoulos, J. Seppälä, E. Kokko and S. Vijay, *Macromol. React. Eng.*, 2013, **7**, 193.
45 E. Nies and A. Stroeks, *Macromolecules*, 1990, **23**, 4088.
46 A. Stroeks and E. Nies, *Macromolecules*, 1990, **23**, 4092.
47 C. I. Poser and I. C. Sanchez, *Macromolecules*, 1981, **14**, 361.

